



DEVELOPMENT AND VALIDATION OF A TRACK BICYCLE INSTRUMENT FOR TORQUE MEASUREMENT USING THE ZIGBEE WIRELESS SENSOR NETWORK

Sadik Kamel Gharghan^{a, b, *}, Rosdiadee Nordin^a, and Mahamod Ismail^a

^a Department of Electrical, Electronic and System Engineering, Faculty of Engineering and Built Environment, Universiti Kebangsaan Malaysia, 43600 UKM Bangi, Selangor, Malaysia

^b Department of Medical Instrumentation Engineering Techniques, Electrical Engineering Technical College, Middle Technical University (MTU), Baghdad-Iraq

Emails: *sadiq_gharghan@yahoo.com, adee@ukm.edu.my (R.N.), mahamod@ukm.edu.my (M.I.)

Submitted: Oct. 16, 2016

Accepted: Feb. 5, 2017

Published: Mar. 1, 2017

Abstract- This study evaluates the consistency between the bicycle torque of the proposed system, and a Schoberer Rad Messtechnik (SRM) system. The torque was measured while a trainer was cycling indoors, and the measured values were compared with those of the SRM system. A Bland-Altman statistical analysis indicated that the measured values agreed with the SRM within 95%. The mean absolute percentage error and root mean square error between the measurements of the proposed system and the SRM system were 8.25%, and 1.86, respectively. The results show that the bicycle torque can be measured accurately and transmitted using ZigBee wireless protocol.

Index terms: measurement accuracy, sensor, statistical analysis, strain gauge, torque, track cycling, wireless sensor network, ZigBee.

I. INTRODUCTION

Track cycling is a sport that has received considerable attention in recent years. The physiological and biomechanical parameters of the bicycle and cyclist, such as pulse rate, speed, cadence, and torque, can be monitored by sensors. These parameters can be transmitted wirelessly in real time to the cyclist or to the coach to provide information about the performance of the bicycle and the cyclist. In track cycling, measuring power while cycling is a crucial factor in assessing the performance of the athletes. Many cyclists and coaches are interested in the mechanical power of the bicycle that is generated during cycling [1]. The cyclists always plan to produce the maximum power output for long durations, where the power delivered to the crank arms is converted to bicycle motion [2]. The cyclist's power can be measured using a device known as a power meter, which often relies on the pedal torque or crank arm torque measurements. Due to recent technological developments, bicycle power meters are becoming part of the training equipment of professional cyclists and are used by cyclists to improve their training [3]. The cyclist's power mainly depends on the torque. The torque that is generated by a cyclist during the crank arm rotation is considered to be the most critical performance index for competitive cyclists because the cyclist's power output can provide precise and accurate measurements of the cyclist's performance and fitness. Neither speed nor heart rate can be used to improve the cyclist's performance because the speed depends on the road grade, wind velocity, terrain, and the athlete's physical characteristics, such as muscle and heart rate, which are controlled by the athlete's current health, diet, and fatigue [4]. The crank torque can be determined by the product of the perpendicular force (F_e) that is applied to the crank arm and the length of the crank arm: $\text{Torque (N.m)} = F_e \times \text{crank arm length}$ [5]. Consequently, the bicycle's power output (W) can be calculated based on the torque measurements; i.e., power output, $W = \text{Torque (N.m)} \times \text{pedal angular velocity (rad.s}^{-1}\text{)}$ [6]. The bicycle's crank arm torque can be monitored wirelessly using a wireless sensor node as a part of the bicycle's wireless sensor network (WSN).

The sensor node architecture is based on four strain gauge sensors and an instrumentation amplifier, magnetic sensor, Arduino Nano microcontroller, and XBee series 2. The system depends on torque measurements taken on the right crank arm using the four strain gauges. The strain gauges form a Wheatstone bridge that is glued to the right crank arm. The measured data of the applied torque on the right crank arm are transmitted wirelessly to the coach based on XBee

series 2 communications. Strain gauges are used to keep system weight loss, which is an important factor in track cycling. However, the position of the strain gauges on the crank arm is critical, and the point of measurement must experience the maximum deformation of the crank arm. The contributions of this paper are to:

- (1) Present a prototype wireless bicycle torque measurement system.
- (2) Compare the results that were obtained with the SRM system, which is a consumer-ready cycling performance monitoring system.
- (3) Validate the proposed system using a statistical analysis to compare it to the SRM.
- (4) Aggregate the torque data by transmitting the average of 60 values, which are collected during each crank arm rotation. In this case, the sensor node does not need to send all of the sensed data; only the average value of every crank arm rotation are sent. The energy consumption can be greatly decreased by reducing the RF communications.

II. RELATED WORK

Torque measurements have been used in several research studies, and several manufacturers provide commercial products. The most common commercially available product to monitor bicycle power is the Schoberer Rad Messtechnik (SRM) [7, 8]. The SRM power meter measures the net torque between the left and right cranks based on a strain gauge. The cyclist's power can be computed by multiplying the torque by the cadence, which is measured by a magnetic sensor (reed switch) that generates a train of pulses. Several other products have also been used to assess cyclist performance. The Power Tap (PT) products measure the torque in the hub of the bicycle's rear wheel using strain gauges [4]. The Ergomo Pro (EP) system employs two optoelectronic sensors that are located in the bottom bracket. The torque is calculated in the left crank arm from the torsion that is produced in the bottom bracket. Hence, only the power that is produced by the left limb can be measured. The total output power can be calculated by multiplying the estimated torque on the left crank arm by two; this assumes that the cyclist's limbs produce nearly identical amounts of power [3]. The POLAR products measure the power based on the bicycle's chain speed and tension. The Garmin Vector measures the power from both the right and left legs that are applied to the bicycle pedal. The Brim Brothers Zone measures the force applied to both pedals based on force sensors that are fixed under the cleats of the shoes. Finally, iBike uses the

sum of the calculated forces that the cyclist faces during cycling using several sensors, such as a wind speed sensor, accelerometer, barometric pressure sensor, and wheel speed and cadence sensors. All of these products are based on the ANT+ wireless protocol.

Table 1 summarizes the previous research on methods of measuring bicycle power that are based on torque or force measurements. A review of these studies demonstrates several limitations and gaps related to wireless bicycle torque measurement that represent challenges in measuring torque:

- (1) Most of the previous studies used consumer-ready devices to measure torque and had no customization and flexibility of the power measurements for off the track analysis by coaches and athletes,
- (2) None of the proposed systems were validated with a consumer-ready device to evaluate the results,
- (3) The consumer-ready cycling performance monitoring systems (i.e., SRM, Garmin Vector, and Power-Tape) do not monitor the torque measurements on the track but instead measure the power,
- (4) The coach cannot monitor the bicycle torque in real time; this means that no data are transmitted in real time between the coach and the cyclist, and
- (5) Some of the previous studies have shortcomings, such as wired connections between the torque measurement unit and the monitoring device, a large size, heavy weight, and a complex hardware design.

These drawbacks motivated us to develop a prototype wireless bicycle torque measurement system that is based on strain gauges. The prototype is characterized by low power consumption because it utilizes low-power wireless technology (i.e., ZigBee), allows real-time data transfer between the cyclist and coach, and the collected data can be evaluated with other systems by storing the acquired data in a data acquisition system.

III. SYSTEM ARCHITECTURE

The proposed wireless sensor network for the torque measurement system is shown in Figure 1. It consists of a torque sensor node and a coordinator node. The torque sensor node comprises several components: a magnetic sensor, a small permanent magnet, a microcontroller that is

embedded in an Arduino Nano board, an instrumentation amplifier, ZigBee (XBee series 2) modules, and a 3.7 V/1200 mAh lithium battery. The coordinator node consists of an Arduino Mega 2560 board, an XBee series 2, and a laptop to monitor the torque data in real time and to compare that data with the SRM system.

Table 1: Previous studies of bicycle torque measurement

Authors	Platform type	Data transmission technology	Measured parameter related to bicycle power	Location of sensor	Sensor used	Advantage of study	Disadvantages of study
Drouet et al. [9]	Instrumented pedals	Wire connection	Applied force	Left and right pedals	Strain gauge	Accurate measurements	<ul style="list-style-type: none"> - Wired connections - Weight of data acquisition system is 1.2 kg - Did not validate with another system
Paul Barratt [10]	Modification of the SRM	Wire connection	Bicycle power	Chainring	Strain gauge	Measures the torque at the initial phase of pedaling	<ul style="list-style-type: none"> - Large size - Additional weight
Spagnol et al.[11]	Used the commercial THUN X-CELL RT pedal sensor	N/C	Torque	Left pedal	Hall sensor with torsion element	Exploit a high correlation measurement between the left and right torques	<ul style="list-style-type: none"> - Not developed for a wireless system - Used a consumer-ready device that was not produced by the authors - Did not validate with another system
Bibbo et al. [12]	Designed by the authors	Bluetooth	Applied force	Between the pedal frame and the clipless	Strain gauge	The instrumented pedal can be fitted to any kind of bicycle	<ul style="list-style-type: none"> - Short communication range - High power consumption - Did not validate with other system
Vanwall-eghem et al. [13]	Designed by the authors	Bluetooth	Applied force	Right pedal	Strain gauge	The force pattern was obtained from one revolution	<ul style="list-style-type: none"> - Short communication range - Did not validate with another system
Dorel et al. [14]	Instrumented pedals	Wire connection	Applied force	Left and right pedal	Strain gauge	Normal and tangential forces applied to the pedals were measured	<ul style="list-style-type: none"> - Heavy weight of the Camelbak bag carried by the cyclist, which contains the data acquisition system - Did not validate with another system
Koutny et al. [15]	Designed by the authors	Wireless system	Applied force	Crank arm	Strain gauge	<ul style="list-style-type: none"> - Better performance during long races - Strain gauges installation based on a finite element analysis of the crank 	<ul style="list-style-type: none"> - Did not validate with another system
Alexandre Balbinot et al. [16]	Designed by the authors	Bluetooth	Applied force	Crank arm	Strain gauge	<ul style="list-style-type: none"> -Measurements of three-dimensional force - Strain gauges installation based on a finite element analysis of the crank 	<ul style="list-style-type: none"> - Did not validate with another system - Complex hardware

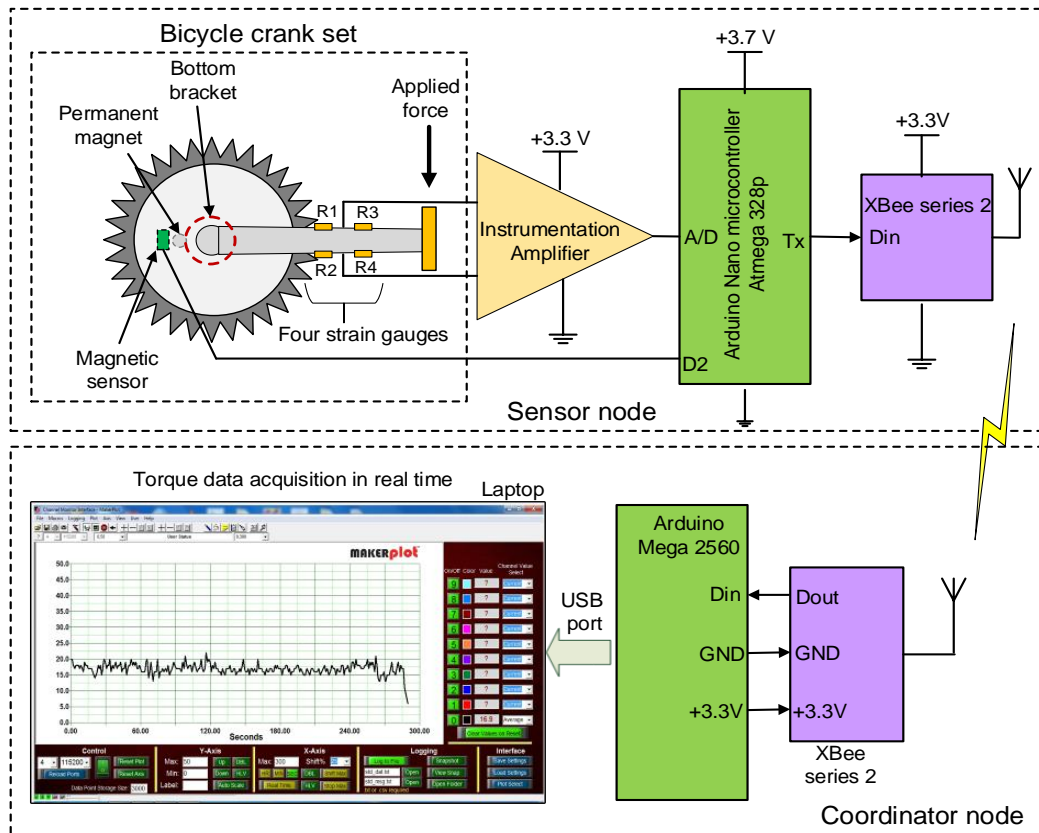


Figure 1. Schematic diagram of the proposed WSN for the torque measurement system

IV. HARDWARE IMPLEMENTATION

The hardware implementation is described in Sections a through c.

a. STRAIN GAUGE SENSOR INSTALLATION on the CRANK ARM

The strain gauge is a type of sensor or transducer that can convert a mechanical force into an electronic signal. Strain gauges are commonly utilized to measure and record torque that is applied to a rotating system. The strain gauge's zero point is affected by changes in temperature, which will produce a measurement error. A Wheatstone bridge is helpful for overcoming this error and provides accurate measurements. Four strain gauges (R_1 , R_2 , R_3 , and R_4) are used to form a Wheatstone bridge to measure the applied torque on the bicycle's right crank arm as shown in Figure. 1. The Wheatstone bridge's output voltage (V_{out}) can be formulated as in equation (1) [17].

$$V_{out} = \left(\frac{R_1}{R_1 + R_2} - \frac{R_4}{R_3 + R_4} \right) V_{in} \quad (1)$$

The output voltage of the Wheatstone bridge is zero when

(i) $R_1 R_3 = R_2 R_4$ and

(ii) All of the resistances have the same value (i.e., $R_1 = R_2 = R_3 = R_4$).

Changes in temperature will also change the gauge's resistance $R_n = R_n + \Delta R_n$ ($n=1, 2, 3,$ and 4), so

$$\frac{V_{out}}{V_{in}} = \frac{1}{4} \left(\left(\frac{\Delta R_1}{R_1} \right) - \left(\frac{\Delta R_2}{R_2} \right) + \left(\frac{\Delta R_3}{R_3} \right) - \left(\frac{\Delta R_4}{R_4} \right) \right) \quad (2)$$

where $\Delta R/R$ is the gauge factor, which represent the sensitivity of the change in strain gauge resistance to the applied strain. Therefore, this term is replaced by

$$\frac{\Delta R}{R} = k \cdot \varepsilon \quad (3)$$

where ε is the strain, and k is the k -factor of the strain gauge [18]. This gives:

$$\frac{V_{out}}{V_{in}} = \frac{k}{4} (\varepsilon_1 - \varepsilon_2 + \varepsilon_3 - \varepsilon_4) \quad (4)$$

where $\varepsilon_1, \varepsilon_2, \varepsilon_3,$ and ε_4 are the strains associated with resistance 1, resistance 2, resistance 3, and resistance 4, respectively.

This experiment used a V-shaped strain gauge of $1400 \Omega \pm 0.3$. This type of strain gauge was selected because it is more appropriate for torque measurements and is suitable for installation on the surface of aluminum materials [19]. The output of the Wheatstone bridge strain gauge is amplified by the instrumentation amplifier AD 623 with an amplifier gain of 46 dB. The output voltage of the amplifier is offset or shifted by $V_{supply}/2$ to ensure that it is within the microcontroller's range. The output of the amplifier is logged by the 10-bit analog-to-digital (A/D) converter that is embedded in the ATmega 328p microcontroller. An RS 473-461 epoxy was used to glue the four strain gauges onto the upper and lower sides of the bicycle crank arm. The strain gauges, which are configured as Wheatstone bridge circuits, are located between the chain ring and crank pedal as shown in Figure 2.

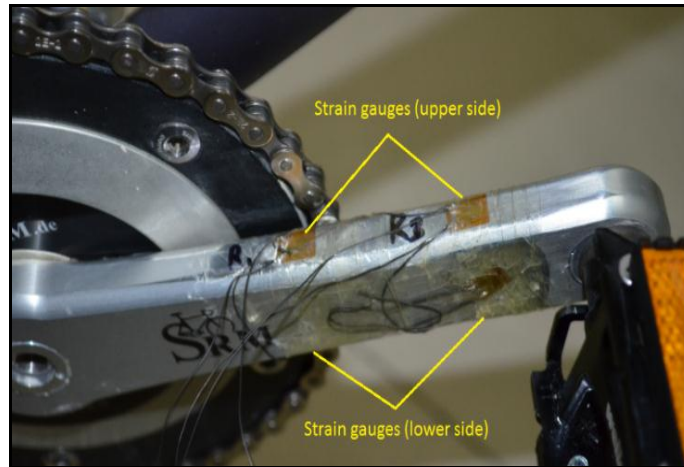


Figure 2. Installation of the strain gauges on the crank arm: upper side and lower side

b. MICROCONTROLLER

The Arduino platform, which is based on the Atmel ATmega microcontroller, is widely used in several applications, such as building automation systems [20], smart grids [21], smart home controls [22], healthcare monitoring [23], and sports performance monitoring [24]. Arduino is commonly used because it is an open-source specification with several different versions, which makes it appropriate for experimental projects [25]. An 8-bit 16 MHz ATmega 328p microcontroller that is embedded in the Arduino Nano board is adopted in this study. It has 32 KB of flash memory, 1 KB of SRAM [26], [27], an 8 channel 10-bit analog to digital converter (ADC), 14 digital input/output pins with six that provide PWM, a USB connection, an SPI interface, a serial port, and operates at 5 volts from a battery or power jack. The Arduino can be programmed in a language that is similar to C++ with some modifications and simplifications, and the essential libraries of Arduino have been written in C and C++ [28]. In this study, the Arduino is programmed to forward the data from the strain gauge sensors to the XBee series 2 module. An Arduino Nano is used to (i) acquire and process the torque data from the strain gauge sensors, (ii) aggregate the torque data at a sampling rate of 200 Hz [29] for each crank arm revolution and average the torque data, (iii) transmit the torque data in the form of a frame via the serial port to the XBee module at 115,200 bps, and (iv) put the XBee module in sleep mode when no torque data are ready for transmission, which significantly reduces the power consumption of the XBee model. These tasks of the Arduino Nano microcontroller were written in the Arduino IDE software version 1.0.6 [30] and were loaded onto the microcontroller as described in Algorithm 1 in Section V.

c. ZIGBEE WIRELESS PROTOCOL

Several wireless technologies that operate at 2.4 GHz can be used in wireless sensor networks, such as Bluetooth, ANT, and ZigBee. Bluetooth and ANT have low communication ranges of 10 [31] and 30 meters, respectively, whereas Zigbee has a relatively long transmission range of approximately 100 meters [32]. ANT consumes less power than Zigbee and Bluetooth. Recently, the demand for the ZigBee wireless protocol has increased, and it is widely used in WSNs. Several studies have shown that WSNs can be made self-healing and self-configurable [33]. The ZigBee protocol will be used in this study because it has a low data rate [34], low power consumption [35], it is small and inexpensive [36], can be configured rapidly, has a suitable communication range [37], and supports multiple network topologies, such as star, point-to-point, and mesh networks with up to 65,000 nodes per network. The Zigbee wireless technology is more appropriate for indoor and outdoor cycling training than Bluetooth and ANT in terms of communication range and is more suitable than Bluetooth in terms of power consumption.

V. SOFTWARE IMPLEMENTATION

An experiment, which consisted of more than seven minutes of cycling with a track bike attached to a Tacx Cycle trainer, was conducted several times under indoor conditions. A manual load was applied to the rear wheel of the bicycle for the torque test. A total of $N = 458$ samples (one sample per crank arm rotation) of the torque were collected by the proposed system and the SRM system. When the cyclist started pedaling from the 0° position (Figure. 3), the magnetic sensor passed by a permanent magnet, which was fixed under the bottom bracket. The permanent magnet energized the magnetic sensor to send a control signal to the microcontroller to start the torque measurement. The torque in the crank arm is proportional to the output voltage of the Wheatstone bridge strain gauge, which is proportional to the force applied by the cyclist to the pedal of the crank arm. The torque is measured 60 times for every crank arm rotation at a sampling frequency of 200 Hz. The torque measurements are then averaged and transmitted through the XBee module of the torque sensor node to the coordinator node. This procedure will produce accurate measurements and reduce the power consumption of the sensor node by decreasing the amount of RF transmitted data. The generated torque is calculated using a pre-programmed algorithm (Algorithm 1). This algorithm was loaded onto the ATmega328

microcontroller, which is embedded on the Arduino Nano board of the torque sensor node. The microcontroller performs the computation of the torque using equation (7). The torque data received from the coordinator node are plotted in real time every second using the Data Acquisition and Graphical Plotting Software for Microcontrollers (MakerPlot). This software displays the data in a GUI and saves the data in a txt file format [38].

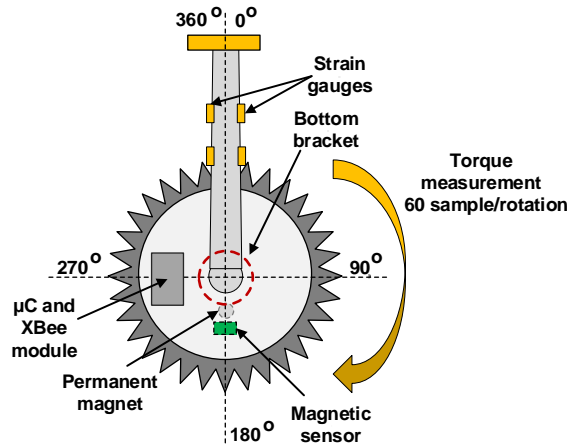


Figure 3. Sensor node components of the torque measurement system installed on the bicycle crank arm and chainring

Algorithm 1: Pseudocode for the proposed torque measurement algorithm

```

1: initially: torque_measurement = 60 times;
2:  setup process {
3:     microcontroller baud rate = 115,200;
4:     Set voltage reference to external reference;
5:     Magnetic sensor output connects to the
       microcontroller
6:  }
7:  Read initial value of the output voltage of the
       strain gauge
8:  void loop() { // main loop
9:    if (magnetic sensor= HIGH) {
10:     Measure the torque for 60 times at a
        sampling rate 200 Hz; // measurement starts
        when the crank arm is at the 0° position
11:     Calculate the average torque;
12:     Send the average torque to the coordinator node;
13:    }
14: } // update the torque measurement

```

VI. TORQUE CALIBRATION

A calibration process is necessary to relate the strain gauge’s output voltage to the applied force on the bicycle crank arm. The calibration was performed by suspending known weights on the end of the bicycle crank arm as shown in Figures 4a and b. A static calibration process was conducted with known weights suspended on the crank arm that varied from 5 Newtons to 85 Newtons in increments of 5 Newtons. The amplified voltage of the strain gauge sensor was recorded with a digital multimeter. The relationship between the applied force F on the crank arm and the output voltage was recorded and plotted (Figure 5) and shows a linear relationship.

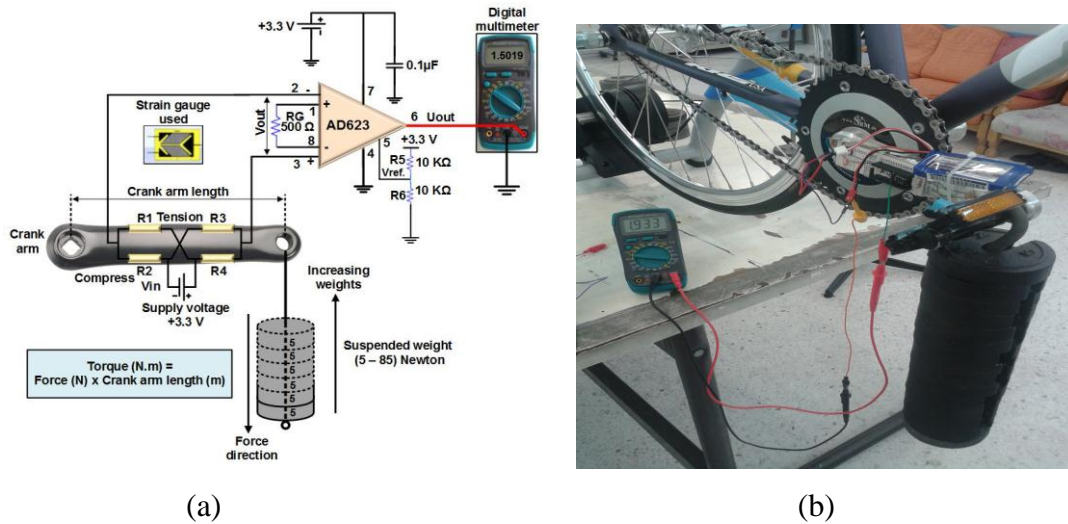


Figure 4. A static torque calibration process using variable weights (5-85 Newtons) suspended by a hook: (a) block diagram and (b) snapshot

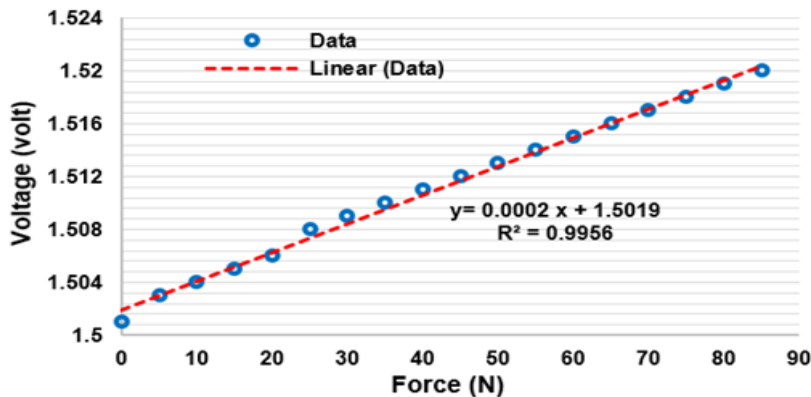


Figure 5. Relationship between the strain gauge’s output voltage and the applied force on the crank arm

Therefore, an approximately linear fit line is plotted through the data points to determine the equation between the applied force and the output voltage:

$$U_{out} = 2 \times 10^{-4} F + 1.5019 \quad (5)$$

where U_{out} is the output voltage of the instrumentation amplifier in volts, F is the applied force on the crank arm in Newtons, and 1.5019 is the offset voltage in volts.

A mathematical relationship between the produced torque and the output voltage can be obtained by multiplying the applied force by the crank arm length (0.17 m was used for the SRM crank arm length in this experiment). Therefore, the produced torque can be expressed as follows:

$$U_{out} = 1.3 \times 10^{-3} T + 1.5019 \quad (6)$$

where T is the torque generated by the crank arm in N.m.

Equation (6) can be rearranged as follows:

$$T = 769.23(U_{out} - 1.5019) \quad (7)$$

Equation (7) can be used in the microcontroller algorithm to measure the torque produced in the bicycle crank arm during pedaling.

VII. EXPERIMENTAL SETUP

Torque measurements can be classified into two classes: static and dynamic torque measurements. A static torque measurement uses several strain gauges that are glued to an axle or shaft as the torque sensor. This is the most common method of measuring torque. Static torque measurements are easier than dynamic torque measurements because the measured axle or shaft is static, whereas it is rotating during dynamic measurements. Therefore, dynamic torque measurements are not easy to perform, and the measured torque is converted into an electrical signal that is transmitted via wireless technologies [39].

This work proposes a system to measure and transmit the torque that is produced in the track bicycle's crank arm due to the force applied to the right crank arm by the cyclist. Four strain gauge transducers that form a Wheatstone bridge were glued to the right crank arm. The electronic system, which consists of the instrumentation amplifier, Arduino Nano, and XBee module, were installed in the middle of the right crank arm. The entire system spins with the crank arm and is controlled by the power applied by the cyclist. The strain gauges were installed

at the points on the crank arm that experienced deformation. The output voltage of the strain gauge was amplified by the AD623 instrumentation amplifier. It is a single supply with a wide voltage range (+3 V to +12 V), low power consumption (0.5 mA at 3 V), and a high common-mode rejection ratio (CMRR) [40] that make it suitable for battery-powered bicycle torque measurements. The gain of the amplifier AG with a single external resistance R_G between pins 1 and 8 (Figure. 4a) can be modeled by equation (8) [41]:

$$A_G = 1 + \frac{100K\Omega}{R_G} \quad (8)$$

where $R_G = 500$ ohm in this experiment; thus, the amplifier gain is 46 dB. It cannot be set to a higher value because the output voltage would be outside the range of the DC supply of the microcontroller (i.e., +3.7 V). The offset voltage can be obtained using a 10 K Ω voltage divider resistor R_5 and R_6 as shown in Figure. 4a. The value of the offset voltage can be calculated from the following equation:

$$V_{offset} = V_{supply} \frac{R_5}{R_5 + R_6} \quad (9)$$

where the supply voltage of the instrumentation amplifier is 3.3 volts; this will produce a theoretical offset voltage of 1.65 volts. This is slightly different from the measured value of 1.5 volts due to the measurement environment. However, the analog output voltage of the amplifier is passed to the A/D converter of the Arduino Nano microcontroller, which acquires the strain gauge's output voltage. The ATmega 328p microcontroller has a 10-bit resolution, which results in 1024 steps from 0 volts to 3.3 volts. For the general case, the VADC step size can be expressed as in equation (10):

$$V_{ADC}_{step} = \frac{V_{reference}}{2^m} \quad (10)$$

where m is the A/D resolution, and $V_{reference}$ is the reference voltage of the A/D converter.

The reference voltage in this experiment is 3.3 volts, so each step will be an increment of 3.222 mV (3.3 volts/1024 steps). The microcontroller prepares the data frame and sends it to the XBee module through the UART port. The baud rate of the microcontroller is set to 115,200 bps; this rate was selected to reduce the transmission time and thus the power consumption of the sensor node. The XBee transmits the torque data over the air to the coordinator node, which is in the same wireless network.

VIII. COMPARISON OF RESULTS AND DISCUSSION

The torque data obtained using the proposed system, which is based on the ZigBee wireless standard, and the SRM system, which is based on the ANT+ wireless protocol, were examined to validate the proposed system. Subsequently, the two systems were compared. The torque and power data from the two systems were recorded every second for the comparison (Figure. 6). The torque data from the SRM system are obtained by calculating the torque from the SRM power measurements; this is because the SRM system cannot measure the torque directly. Figure. 6 shows the torque and power raw data that were reported by each system for more than seven minutes of indoor cycling (i.e., in a laboratory environment). The results show slight differences between the two systems. To examine or test the data obtained by the proposed system, a statistical analysis was conducted.

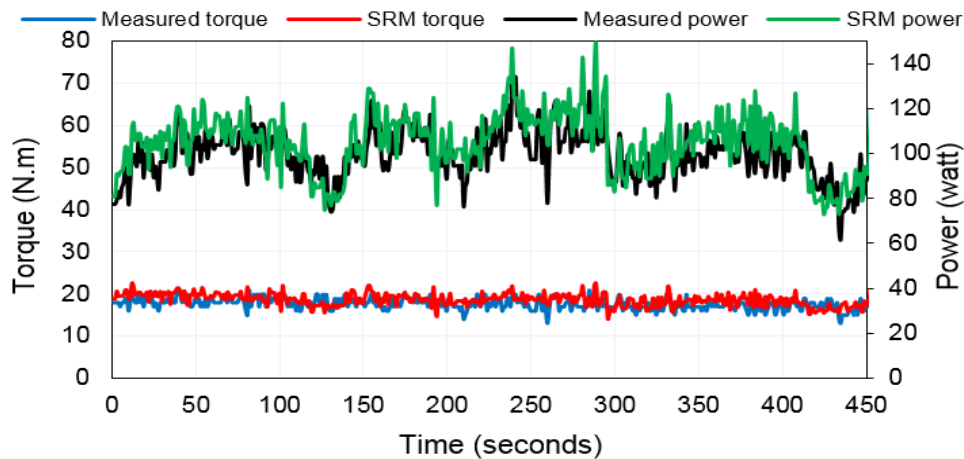


Figure 6. Torque and power data for the proposed system and the SRM system

a. ERROR TEST

The errors and mean absolute percentage error (MAPE) in the torque measurements of the proposed system with respect to those of the SRM system are plotted in Figures 7 and 8, respectively. Figure 7 shows the errors and mean absolute error (MAE), whereas Figure. 8 shows the absolute percentage errors (APE) and MAPE. Both figures vary over the range of 14 to 23 N.m for the SRM torque. Relative to the SRM system, the MAE is 1.55, the MAPE is 8.25%, and the root mean square error (RMSE) is 1.86. The MAPE appears to be relatively high relative to the SRM torque measurement. This error is due to the position of the strain gauges on the crank

arm. The location must be selected carefully to produce the maximum deformation in the crank arm when the force is applied by the cyclist; this procedure requires an extensive finite element analysis.

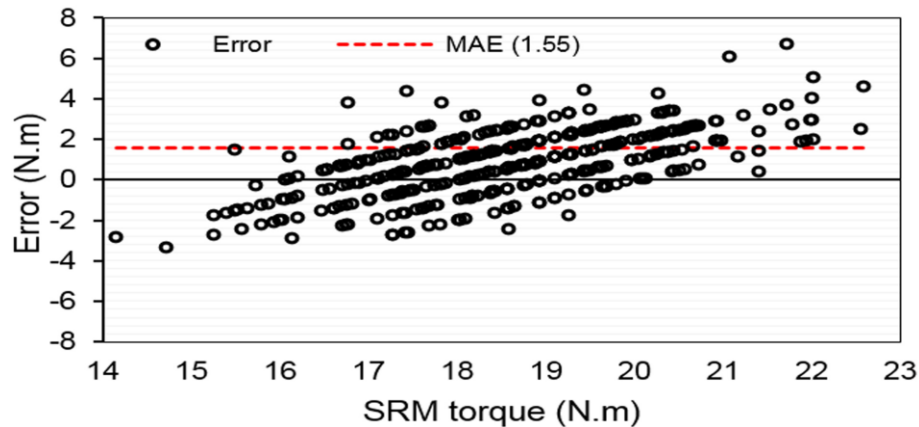


Figure 7. Errors and mean absolute error of the torque measurements

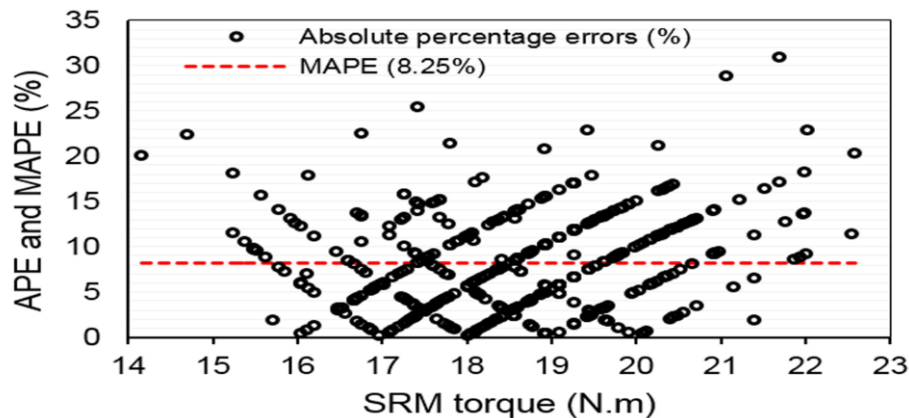


Figure 8. Absolute percentage errors and mean absolute percentage error of the torque measurements

b. BLAND–ALTMAN TEST

The Bland-Altman is a type of statistical analysis that is typically used to compare measurements relative to a reference value. The Bland – Altman plot was used to show the symmetry or differences between the proposed system and the SRM system. Figure. 9 show a Bland – Altman plot of the differences between the proposed system and the SRM system for all of the data that were collected throughout the range of torque. To illustrate the effect of the torque on the difference between the two systems, regression lines (dotted lines) were added to the plot. Most

(435/458) of the differences between the torque data between the proposed system and the SRM system (i.e., errors) were within the $\mu \pm 2\sigma$ (95%) limits of agreement (- 4.15, 2.19). The average or mean difference (bias) of the torque measurements between the proposed system and the SRM system is -0.97. The standard deviation of the difference is 1.585, and the width of the 95% limits of agreement is 6.34.

In studies from the literature [42-45], most of the data lie within the 95% limits of agreement. Therefore, this study is consistent with the previous research. A small amount of torque data lies outside the regression lines; they are shown as diamonds in Figure 9. These errors are also caused by the position of the strain gauges on the crank arm, which was discussed in Section VIII (A). The Bland–Altman test thus revealed relatively good agreement between the two systems.

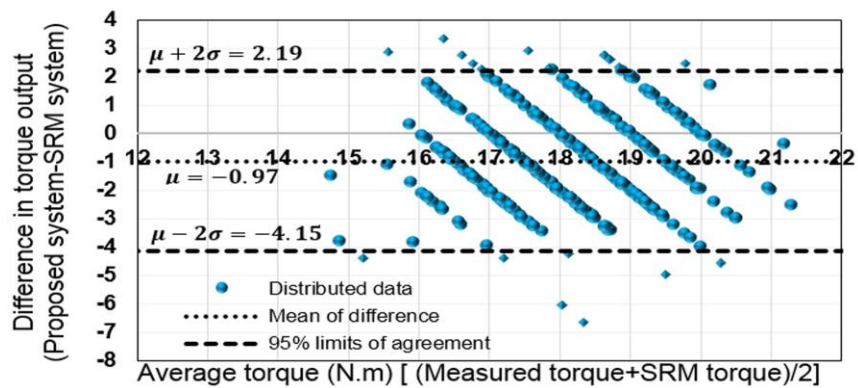


Figure 9. Bland–Altman torque plot (differences between the proposed system and the SRM system) with the 95% limits of agreement (circles), the mean difference, and regression lines (dotted lines). The values represent all 458 torque measurements

c. HISTOGRAM TEST

Histograms are the most popular graphical illustration of a frequency distribution and feature representation [46]. A histogram consists of adjacent rectangles; the y – axis (heights of the rectangles) represents the class frequencies, and the x – axis (bases of the rectangles) represents the successive class boundaries [47]. High bars indicate more points, whereas low bars indicate fewer points in a class. The SRM system uses a histogram for the statistical analysis [48] based on a software package that was developed by SRM to show how often each value of a measured parameter occurred during the test. The SRM histogram shows that the efforts are proceeding as planned. Therefore, it is important to determine whether the data measured by the proposed system are compatible with the SRM system. The histogram of the torque data (Figure. 10)

shows peaks of 131 and 130 points in the 18 and 19 N.m classes for the proposed system and the SRM system, respectively. These results demonstrate that the data measured by the proposed system are comparable with those measured by the SRM system.

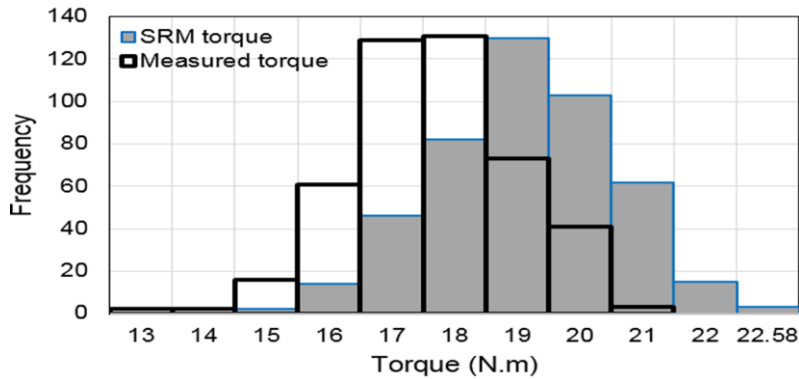


Figure 10. Histogram of the torque data from the proposed system and the SRM system

IX. CONCLUSIONS

This paper presents the design and implementation of a wireless bicycle torque measurement system that is based on the XBee wireless protocol, an Arduino Nano microcontroller, strain gauge transducers, and an amplifier circuit. This study confirmed the close agreement between the data obtained by the proposed system, which is based on the ZigBee (XBee series 2) wireless standard technology, and those obtained by the SRM system, which is based on the ANT+ wireless protocol. Small differences were noted between the two systems. The statistical analysis (i.e., MAE, MAPE, RMSE, histogram, and Bland–Altman test) provided strong evidence of the validity of the proposed system. Future work will focus on reducing the measurement error by selecting the most appropriate locations for the strain gauges on the bicycle crank arm based on finite element analysis.

ACKNOWLEDGMENTS

This work was supported by Malaysia's Ministry of Education, under Sports Engineering Grant with ref. No: PKT1/2013 and Universiti Kebangsaan Malaysia with grant ref. No: INOVASI-2014-015.

REFERENCES

- [1] M. Corno, D. Berretta, P. Spagnol, and S. M. Savaresi, "Design, control, and validation of a charge-sustaining parallel hybrid bicycle," *IEEE T. Contr. Syst. T.*, vol. 24, pp. 817-829, 2016.
- [2] R. Bini and F. Carpes, "Measuring Pedal Forces," in *Biomechanics of Cycling*, R. R. Bini and F. P. Carpes, Eds., ed: Springer International Publishing, 2014, pp. 13-21.
- [3] R. Tielert, N. Wehn, T. Jaitner, and R. Volk, "Power Measurement in Cycling using inductive Coupling of Energy and Data (P80)," in *The Engineering of Sport 7*, ed: Springer Paris, 2008, pp. 397-403.
- [4] G. E. F. Pawelka, "The innovation equation: balancing clever technical solutions with users' needs," *Procedia Eng.*, vol. 2, pp. 2613-2617, 2010.
- [5] O. V. Casas, R. Dalazen, and A. Balbinot, "3D load cell for measure force in a bicycle crank," *Measurement*, vol. 93, pp. 189-201, 2016.
- [6] S. K. Gharghan, R. Nordin & M. Ismail. Empirical investigation of pedal power calculation techniques for track cycling performance measurement. *IEEE Student Conference on Research and Development (SCORED)*. pp. 48-53, 2013.
- [7] B. Wainwright, C. Brian Cooke, and J. Paul O'Hara, "The validity and reliability of a sample of 10 Wattbike cycle ergometers," *J. Sport. Sci.*, pp. 1-8, 2016.
- [8] L. Rylands, S. J. Roberts, M. Cheetham, and A. Baker, "Velocity production in elite BMX riders: a field based study using a SRM power meter," *Journal of Exercise Physiology Online*, vol. 16, pp. 40-50, 2013.
- [9] J.-M. Drouet, Y. Champoux, and S. Dorel, "Development of Multi-platform Instrumented Force Pedals for Track Cycling (P49)," in *The Engineering of Sport 7*, ed: Springer Paris, 2008, pp. 263-271.
- [10] P. Barratt, "SRM Torque Analysis of Standing Starts in Track Cycling (P85)," in *The Engineering of Sport 7*, ed: Springer Paris, 2008, pp. 443-448.
- [11] P. Spagnol, M. Corno, and S. Savaresi, "Pedaling torque reconstruction for half pedaling sensor," in *Proc. IEEE European Control Conference (ECC)*, 2013, pp. 275-280.
- [12] D. Bibbo, S. Conforto, I. Bernabucci, M. Schmid, and T. D'Alessio, "A wireless integrated system to evaluate efficiency indexes in real time during cycling," in *Proc. 4th European*

- Conference of the International Federation for Medical and Biological Engineering. vol. 22, J. Vander Sloten, P. Verdonck, M. Nyssen, and J. Haueisen, Eds., ed: Springer Berlin Heidelberg, 2009, pp. 89-92.
- [13] J. Vanwalleghem, F. Mortier, I. De Baere, M. Loccufier, and W. Van Paepegem, "Instrumentation of a racing bicycle for outdoor field testing and evaluation of the cyclist's comfort perception," in Proc. 15th International Conference on Experimental Mechanics (ICEM15), July 2012, pp. 1-12.
- [14] S. Dorel, J. M. Drouet, F. Hug, P. M. Lepretre, and Y. Champoux, "New instrumented pedals to quantify 2D forces at the shoe-pedal interface in ecological conditions: preliminary study in elite track cyclists," *Comput. Methods Biomech. Biomed. Eng.*, vol. 11, pp. 89-90, 2008.
- [15] D. Koutny, D. Palousek, P. Stoklasek, J. Rosicky, L. Tepla, M. Prochazkova, et al., "The Biomechanics of Cycling with a Transtibial Prosthesis: A Case Study of a Professional Cyclist," *International Journal of Medical, Health, Biomedical, Bioengineering and Pharmaceutical Engineering*, vol. 7, pp. 537-542, 2013.
- [16] A. Balbinot, C. Milani, and J. d. S. B. Nascimento, "A New Crank Arm-Based Load Cell for the 3D Analysis of the Force Applied by a Cyclist," *Sensors*, vol. 14, pp. 22921-22939, 2014.
- [17] W. C. Ang, P. Kropelnicki, J. M. L. Tsai, K. C. Leong, and C. S. Tan, "Design, Simulation and Characterization of Wheatstone Bridge Structured Metal Thin Film Uncooled Microbolometer," *Procedia Eng.*, vol. 94, pp. 6-13, 2014.
- [18] K. Hoffmann, *An Introduction to Stress Analysis and Transducer Design using Strain Gauges*, 2012.
- [19] Strain gauges absolute precision from HBM. Available:<http://www.hbm.com/fileadmin/mediapool/hbmdoc/technical/s1265.pdf> (accessed on 20 September 2014).
- [20] M. d. C. Curras-Francos, J. Diz-Bugarin, J. R. Garcia-Vila, and A. Orte-Caballero, "Cooperative Development of an Arduino-Compatible Building Automation System for the Practical Teaching of Electronics," *IEEE-RITA*, vol. 9, pp. 91-97, 2014.
- [21] N. C. Batista, R. Melício, and V. M. F. Mendes, "Layered Smart Grid architecture approach and field tests by ZigBee technology," *Energy Conv. Manag.*, vol. 88, pp. 49-59, 2014.

- [22] K.-Y. Lian, S.-J. Hsiao, and W.-T. Sung, "Smart home safety handwriting pattern recognition with innovative technology," *Comput. Electr. Eng.*, vol. 40, pp. 1123-1142, 2014.
- [23] H. Kemis, N. Bruce, P. Wang, T. Antonio, G. Lee Byung, and L. Hoon Jae, "Healthcare monitoring application in ubiquitous sensor network: Design and implementation based on pulse sensor with arduino," in *Proc. IEEE 6th International Conference on New Trends in Information Science and Service Science and Data Mining (ISSDM)*, Taipei, 2012, pp. 34-38.
- [24] N. S. A. Zulkifli, F. K. C. Harun, and N. S. Azahar, "XBee wireless sensor networks for Heart Rate Monitoring in sport training," in *Proc. IEEE International Conference on Biomedical Engineering (ICoBE)* Penang, Malaysia, 2012, pp. 441-444.
- [25] Y. F. Solahuddin and W. Ismail, "Data fusion for reducing power consumption in Arduino-XBee wireless sensor network platform," in *Proc. IEEE International Conference on Computer and Information Sciences (ICCOINS)*, Kuala Lumpur, Malaysia, 2014, pp. 1-6.
- [26] D. Djenouri, N. Merabtine, F. Z. Mekahlia, and M. Doudou, "Fast distributed multi-hop relative time synchronization protocol and estimators for wireless sensor networks," *Ad Hoc Netw.*, vol. 11, pp. 2329-2344, 2013.
- [27] C. Bell, *Beginning Sensor Networks with Arduino and Raspberry Pi: Apress Media*, 2013.
- [28] V. Georgitzikis, O. Akribopoulos, and I. Chatzigiannakis, "Controlling Physical Objects via the Internet using the Arduino Platform over 802.15.4 Networks," *IEEE Latin America Trans. (Revista IEEE America Latina)*, vol. 10, pp. 1686-1689, 2012.
- [29] T. Paul J., C. Stuart J., E. Tammie R., G. A. Scott, and K. Justin G., "Comparison of ergometer- and track-based testing in junior track-sprint cyclists. Implications for talent identification and development," *J. Sport. Sci.*, pp. 1-7, 2016.
- [30] Arduino IDE. Available: <http://arduino.cc/en/Main/Software> (accessed on 3 January 2014).
- [31] G. Kiokes, C. Vossou, P. Chatzistamatis, S. M. Potirakis, S. Vassiliadis, K. Prekas, et al., "Performance Evaluation of a Communication Protocol for Vital Signs Sensors Used for the Monitoring of Athletes," *Int. J. Distrib. Sens. Netw.*, vol. 2014, p. 13, 2014.
- [32] S. K. Gharghan, R. Nordin & M. Ismail. A Survey on Energy Efficient Wireless Sensor Networks for Bicycle Performance Monitoring Application. *J. Sensors* vol. 2014, pages 16, 2014.

- [33] Jun Yu and Xueying Zhang, "A Cross-Layer Wireless Sensor Network Energy-Efficient Communication Protocol for Real-Time Monitoring of the Long-Distance Electric Transmission Lines," *J. Sensors*, Article ID 515247, in press, 2015.
- [34] J. Hughes, J. Yan, and K. Soga, "Development of wireless sensor network using bluetooth low energy (BLE) for construction noise monitoring," *International Journal on Smart Sensing and Intelligent Systems*, vol. 8, pp. 1379-1405, 2015.
- [35] S. K. Gharghan, R. Nordin, M. Ismail & J. Abd Ali. Accurate Wireless Sensor Localization Technique based on Hybrid PSO-ANN Algorithm for Indoor and Outdoor Track Cycling. *IEEE Sens. J.*, vol. 16, pp. 529 - 541, 2016.
- [36] N. K. Suryadevara, S. C. Mukhopadhyay, S. D. T. Kelly, and S. P. S. Gill, "WSN-Based Smart Sensors and Actuator for Power Management in Intelligent Buildings," *IEEE/ASME Trans. Mechatronics*, vol. 20, pp. 564-571, 2015.
- [37] W.-T. Sung, J.-H. Chen, and C.-L. Hsiao, "Data fusion for PT100 temperature sensing system heating control model," *Measurement*, vol. 52, pp. 94-101, 2014.
- [38] Data Acquisition and Graphical Plotting Software for Microcontrolles (MakerPlot). Available: <http://www.makerplot.com> (accessed on 3 March 2014).
- [39] C.-J. Lin, C. R. Lin, S.-K. Yu, G.-X. Liu, C.-W. Hung, and H.-P. Lin, Applied measurement system. In *Study on Wireless Torque Measurement Using SAW Sensors: InTech*, 2012.
- [40] F. N. Guerrero, E. M. Spinelli, and M. A. Haberman, "Analysis and Simple Circuit Design of Double Differential EMG Active Electrode," *IEEE T Biomed. Circ. S.*, vol. 10, pp. 787-795, 2016.
- [41] A. Ali, M. R. Mughal, H. Ali, and L. Reyneri, "Innovative power management, attitude determination and control tile for Cube Sat standard Nano Satellites," *Acta Astronaut.*, vol. 96, pp. 116-127, 2014.
- [42] L.-T. Yang, Y. Nagata, K. Otani, Y. Kado, Y. Otsuji, and M. Takeuchi, "Feasibility of one-beat real-time full-volume three-dimensional echocardiography for assessing left ventricular volumes and deformation parameters," *J. Am. Soc. of Echocardiog.*, vol. 29, pp. 853-860, 2016.
- [43] A. Ferrari, P. Ginis, M. Hardegger, F. Casamassima, L. Rocchi, and L. Chiari, "A Mobile Kalman-Filter Based Solution for the Real-Time Estimation of Spatio-Temporal Gait Parameters," *IEEE T. Neur. Sys. Reh.*, vol. 24, pp. 764-773, 2016.

- [44] S. K. Gharghan, R. Nordin & M. Ismail 2015. Statistical validation of performance of ZigBee-based wireless sensor network for track cycling. International Conference on Smart Sensors and Application (ICSSA), pp. 44-49, 2015.
- [45] S. M. Rodger, D. J. Plews, J. McQuillan, and M. W. Driller, "Evaluation of the Cyclus cycle ergometer and the Stages power meter for measurement of power output in cycling, Journal of Science and Cycling, vol. 5, pp. 16-22, 2016.
- [46] C. Lee, H. C. Shin, S. Kang, and J.-B. Lee, "Measurement of desirable minimum one-way bike lane width," KSCE J. Civ. Eng., vol. 20, pp. 881-889, 2016.
- [47] R. A. Johnson, I. Miller, and J. E. Freund, Probability and statistics for engineers: Prentice-Hall, 2011.
- [48] A.Wooles. SRM user manual 6th edition, 2010. Available: <http://www.srm.de> (accessed on 8 July 2014).